

Elimination of influence of neutron-skin size difference of initial colliding nuclei in Pb+Pb collisions

Gao-Feng Wei^{1,2,3,*}

¹*Department of Applied Physics, Xi'an JiaoTong University, Xi'an 710049, China*

²*School of Physics and Mechatronics Engineering,*

Xi'an University of Arts and Science, Xi'an, 710065, China

³*Department of Physics and Astronomy, Texas A&M University-Commerce, Commerce, TX 75429-3011, USA*

Within an isospin- and momentum-dependent transport model using as an input nucleon density profiles from Hartree-Fock calculations based on a modified Skyrme-like (MSL) model, we study how to eliminate the influence of neutron-skin size difference of initial colliding nuclei in probing the nuclear symmetry energy. Within the current experimental uncertainty range of neutron-skin size of ^{208}Pb , the Pb+Pb collisions are performed in semicentral and peripheral collisions with impact parameters of 5 and 9fm and at beam energies from 50 MeV/nucleon to 1000 MeV/nucleon, respectively. It is shown that combination of neutron and proton collective flows, i.e., neutron-proton differential elliptic flow, neutron-proton elliptic flow difference, neutron-proton differential transverse flow and neutron-proton transverse flow difference, can effectively eliminate the effects of neutron-skin size difference and thus can be as useful sensitive observables in probing nuclear matter symmetry energy in heavy-ion collisions. Moreover, the combined neutron-proton stopping power including the neutron-proton differential stopping power and neutron-proton stopping power difference can also eliminate the effects of neutron-skin size difference and shows some sensitivities to symmetry energy especially at the lower beam energy.

PACS numbers: 25.70.-z, 24.10.Lx, 21.65.-f

I. INTRODUCTION

The density dependence of nuclear symmetry energy $E_{sym}(\rho)$ as one of important issue in isospin physics has been studied for the past few decades because of its very importance not only in understanding the structure of radiative nuclei in nuclear physics [1–4] but also its crucial roles in nuclear astrophysics [5–9]. Up to now, although many useful experimental observables [9–19] have been proposed to determine the nuclear symmetry energy in heavy-ion collisions, they have had limited success because of its sensitivity not only to nuclear symmetry energy but also other poorly known physical effects [20, 21]. Nevertheless, a key step in determining the nuclear symmetry energy is the determination of experimental observables which can be serve as clean and sensitive probes [20, 21]. Therefore, the search of the experimental observables sensitive only to nuclear symmetry energy than others is a crucial task in determination of nuclear symmetry energy.

It is well known that heavy-ion reactions induced by neutron-rich nuclei provide an important opportunity to constrain the symmetry energy in a broad density range [22–27]. To initialize transport models of heavy-ion reactions, it is necessary to know the nucleon density profiles for the two colliding nuclei. Generally speaking, one should use the Thomas-Fermi method to extract the density profiles for the colliding nuclei. Practically, one usually use other methods to approximate Thomas-Fermi

method during initializing the colliding nuclei such as the droplet model used in the isospin-dependent quantum molecular dynamics (IQMD) model [28, 29] and the Skyrme Hartree-Fock model used in the isospin-dependent Boltzmann-Uehling-Uhlenbeck (IBUU) model [30]. In any case, the initialization should guarantee the numerical stabilization of colliding nuclei and fit the bulk nuclei properties as good as possible; see, e.g., Refs.[31, 32]. The main problem of these methods is the numerical stability of initial colliding nuclei in the subsequent reaction. However, this allows one to easily separate effects on the final observables due to the initial state from those due to the reactions [33]. Based on this consideration, by examining the relative effects of neutron-skin size in initial nuclei and the symmetry energy at suprasaturation densities reached in heavy-ion collisions on the charged pion ratio in the final state, we have shown recently that the π^-/π^+ ratio is sensitive not only to nuclear symmetry energy but also the neutron-skin size of initial colliding nuclei especially in peripheral collisions, see Ref. [33]. Nevertheless, as mentioned above a crucial task in determination of symmetry energy is to find the clean experimental observables. Under this consideration in mind, we are going to find which experimental observables are sensitive to nuclear symmetry energy than neutron-skin size difference of initial colliding nuclei. To this end, in this work we investigate how to eliminate the influence of the neutron-skin size difference of initial colliding nuclei in probing the nuclear symmetry energy in Pb+Pb heavy-ion collisions. It can be found later that the combined neutron-proton collective flow and stopping power can effectively eliminate the effects of neutron-skin size difference of initial colliding nuclei

*Email address: wei.gaofeng@foxmail.com

but keep the effects of symmetry energy especially at the lower beam energy.

II. THE MODEL

In this part we briefly describe the model used in the present study, i.e., the isospin- and momentum-dependent Boltzmann-Uehling-Uhlenbeck transport model [30] of version IBUU11 [34]. The momentum dependence of both the isoscalar [35–39] and isovector [30, 40–42] parts of the nuclear interaction is important in understanding not only many phenomena in intermediate-energy heavy-ion collisions but also thermodynamical properties of isospin-asymmetric nuclear matter [43–45]. The mean-field potential for a nucleon with momentum \vec{p} and isospin τ can be written as [40]

$$\begin{aligned}
 U(\rho, \delta, \vec{p}, \tau) = & A_u(x) \frac{\rho_{-\tau}}{\rho_0} + A_l(x) \frac{\rho_\tau}{\rho_0} \\
 & + B \left(\frac{\rho}{\rho_0} \right)^\sigma (1 - x\delta^2) - 8\tau x \frac{B}{\sigma + 1} \frac{\rho^{\sigma-1}}{\rho_0^\sigma} \delta \rho_{-\tau} \\
 & + \frac{2C_{\tau,\tau}}{\rho_0} \int d^3p' \frac{f_\tau(\vec{p}')}{1 + (\vec{p} - \vec{p}')^2 / \Lambda^2} \\
 & + \frac{2C_{\tau,-\tau}}{\rho_0} \int d^3p' \frac{f_{-\tau}(\vec{p}')}{1 + (\vec{p} - \vec{p}')^2 / \Lambda^2}. \quad (1)
 \end{aligned}$$

In the above, $\rho = \rho_n + \rho_p$ is the nucleon number density and $\delta = (\rho_n - \rho_p) / \rho$ is the isospin asymmetry of the nuclear medium; $\rho_{n(p)}$ denotes the neutron (proton) density, isospin τ is 1/2 for neutrons and $-1/2$ for protons, and $f(\vec{p})$ is the local phase space distribution function. The expressions and values of the parameters $A_u(x)$, $A_l(x)$, σ , B , $C_{\tau,\tau}$, $C_{\tau,-\tau}$, and Λ can be found in Refs. [40, 46], and they lead to the binding energy of -16 MeV, incompressibility 212 MeV for symmetric nuclear matter, and symmetry energy $E_{sym}(\rho_0) = 30.5$ MeV at saturation density $\rho_0 = 0.16 \text{ fm}^{-3}$, respectively.

The variable x is introduced to mimic different forms of the symmetry energy predicted by various many-body theories without changing any properties of symmetric nuclear matter and the value of $E_{sym}(\rho_0)$. At suprasaturation densities, although the IBUU calculations favour by comparing with the FOPI data a super soft symmetry energy with $x = 1$ [47], compared to the FOPI data the ImIQMD calculations by Feng *et al* [48] show a super hard symmetry energy. Therefore, to evaluate the relative effects of symmetry energy we use two values of $x = 1$ and $x = 0$ as the so-called soft and stiff symmetry energy parameters as shown in Fig. 1 [33]. It should be mentioned that the current uncertain range of symmetry energy at suprasaturation densities is much larger than the one used here [21, 49]. The density dependence of $E_{sym}(\rho)$ around ρ_0 is generally characterized by the slope parameter $L \equiv 3\rho_0(dE_{sym}/d\rho)_{\rho=\rho_0}$. The softer (stiffer) $E_{sym}(\rho)$ with $x = 1$ ($x = 0$) has a value of $L = 16.4$ (62.1) MeV.

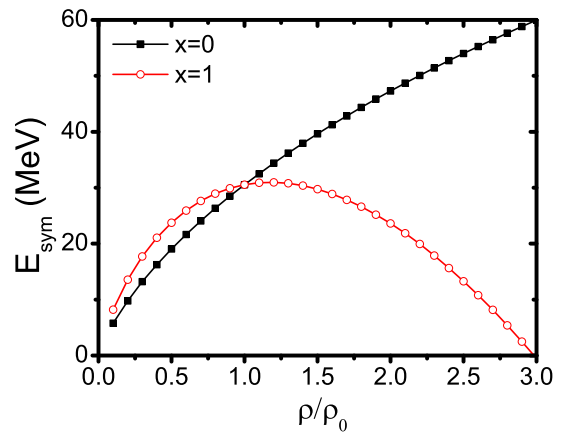


FIG. 1: (Color online) The density dependence of the symmetry energy. Taken from Ref. [33].

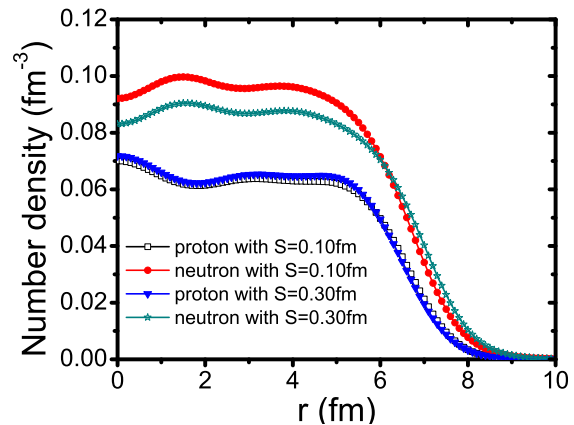


FIG. 2: (Color online) The neutron and proton density profiles for ^{208}Pb with neutron-skin thickness of 0.1 and 0.3 fm, respectively. Taken from Ref. [33].

To examine effects of the neutron-skin size of initial colliding nuclei, we initialize nucleons in phase space using neutron and proton density profiles predicted by Hartree-Fock calculations based on the MSL model [50, 51]. Different values of neutron-skin thickness can be obtained by changing only the value of L in the MSL0 force [51] while keeping all the other macroscopic quantities the same. Shown in Fig. 2 are the density profiles corresponding to a neutron-skin thickness S of 0.1 and 0.3 fm of ^{208}Pb [33], which are in the range of about 0.11 ± 0.06 fm from π^+ -Pb scattering [52] to $0.33^{+0.16}_{-0.18}$ fm from the PREX-1 experiments using parity violating e-Pb scattering [53]. Although these available data suffer from large uncertainties, it was shown very recently within a relativistic mean-field model [54] that a neutron-skin for ^{208}Pb as thick as $0.33 + 0.16$ fm reported by the PREX-I experiment [53] can not be ruled out although most other studies have reported much smaller average values albeit largely overlapping with the PREX-I result within error bars. It is expected that the proton distributions are al-

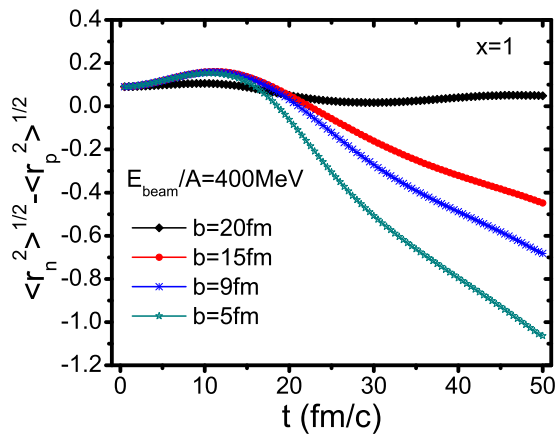


FIG. 3: (Color online) Evolution of the rms radius difference between neutron and proton initially setting as 0.1fm in $^{208}\text{Pb}+^{208}\text{Pb}$ collisions with impact parameters of 5, 9, 15 and 20fm at beam energy of 400MeV/nucleon, respectively.

most identical, while the neutrons distribute differently in the two cases considered.

Before showing the results of the studies, one must check the stability of the ground state nucleus. To this end, one can check the time evolution of the rms radius difference between neutrons and protons in the projectile and/or target with impact parameter to be infinite in the reaction model. This is because when the impact parameter is infinite, the projectile and target can not touch with each other and the corresponding interaction between them becomes zero, they are in their ground states and move along their initial trajectory; it is naturally that the initial rms radius difference between neutrons and protons remains unchanged. Shown in Fig. 3 is the evolution of the rms radius difference between neutrons and protons initially setting as 0.1fm both in the projectile and target for different impact parameters at beam energies of 400MeV/nucleon, respectively. Firstly, it can be found that the value of the rms radius difference between neutrons and protons decreases rapidly with the impact parameter decreasing due to the interactions between the projectile and target as well as the corresponding collisions among nucleons increasing. Secondly, it is expected that the initial rms radius difference between neutrons and protons in the projectile and/or target approximately approaches stable as the impact parameter increasing to be 20fm. Certainly, a long-period and small-amplitude oscillation of the rms radius difference is still seen due to the distance between the projectile and target inadequate far and the tiny fluctuation from collisions between nucleons in the same nucleus. However, this level of stability of the ground state nucleus more or less lasts long enough, which should be reflected in the final reaction production.

III. RESULTS AND DISCUSSIONS

We now present results of the study in the following. Considering that there is no obvious neutron-skin effects in head-on heavy-ion reactions as shown in our previous work [33], we thus carry out this study in semicentral and peripheral $^{208}\text{Pb}+^{208}\text{Pb}$ collisions with impact parameters of 5 and 9fm. On the other hand, to distinguish the difference of neutron-skin size of $S=0.1$ and 0.3fm, we have performed large scale calculations with 4×10^5 events in each case reported here. Thus, the statistical error bars are smaller than the plotting symbols in most plots. In addition, the percentage used in some figure is to avoid too much numerical digit after the decimal.

A. The elliptic flow

The elliptic flow has been widely used to study the properties of the hot and dense matter formed in the early stage of heavy-ion collisions at relativistic and intermediate energies, see, e.g., Refs. [49, 55, 56]. To probe the density dependence of symmetry energy, we show in Fig. 4 and Fig. 5 transverse momentum dependence of elliptic flow of the midrapidity ($|y/y_{beam}| \leq 0.5$) neutrons and protons in semicentral and peripheral $^{208}\text{Pb}+^{208}\text{Pb}$ collisions with impact parameters of 5 and 9fm and at beam energies from 50 to 1000 MeV/nucleon, respectively. It can be found that the elliptic flow of nucleons shows a transition from in-plane to out-of-plane with the beam energy increasing from 50 to 1000MeV/nucleon. This is because at the lower beam energies, the mean field dominates the reaction dynamics and causes the in-plane enhancement of emitted reaction products, while with the beam energies increasing, the mean field becomes less important and the collective expansion process based on nucleon-nucleon scattering starts to be predominant, and the squeezed out elliptic flow as the result of shadowing of spectator starts to become negative [57–59]. However, the symmetry energy effects on elliptic flow of nucleons are not obvious as reported in previous Refs. [20, 60], and the neutron-skin effects on elliptic flow of nucleons are comparable with or larger than that of symmetry energy. Nevertheless, the elliptic flow of both neutron and proton has larger value with thinner neutron-skin due to more nucleons in spectator generating the stronger shadowing effects on in-plane emitted nucleons and leading squeezed out elliptic flow of out-of-plane nucleons to be larger. In other words, the effects of neutron-skin size on elliptic flow of neutron and proton are approximately identical except for the additional Coulomb repulsion between protons. This naturally leads us to check whether combining the neutron and proton elliptic flows can eliminate the effects of neutron-skin size difference but keep the effects of symmetry energy. To this end, we formulate

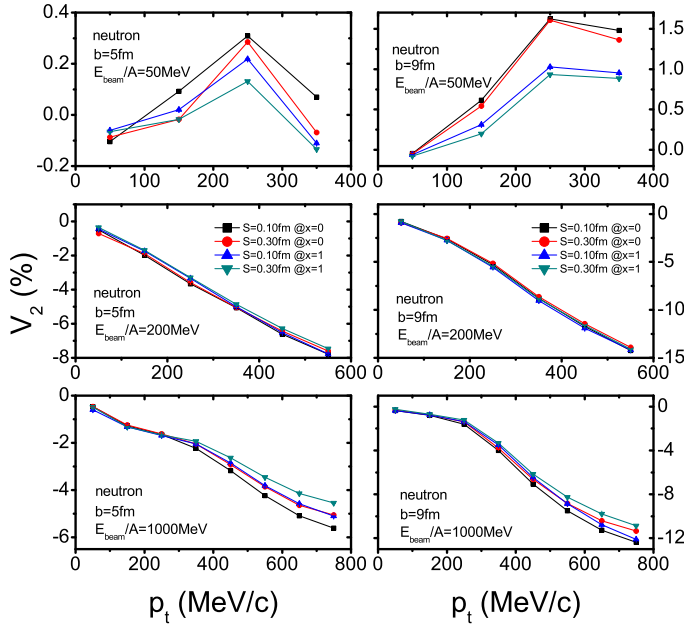


FIG. 4: (Color online) The transverse momentum dependence of elliptic flow of the midrapidity ($|y/y_{beam}| \leq 0.5$) neutrons in semicentral and peripheral $^{208}\text{Pb}+^{208}\text{Pb}$ collisions with impact parameter of 5 and 9 fm and at beam energies from 50 to 1000 MeV/nucleon, respectively.

the so-called neutron-proton differential elliptic flow

$$v_2^{np}(u) = \frac{1}{N(u)} \sum_{i=1}^{N(u)} v_2^i(u) w_i$$

$$= \frac{N_n(u)}{N(u)} \langle v_2^n(u) \rangle - \frac{N_p(u)}{N(u)} \langle v_2^p(u) \rangle, \quad (2)$$

where $N(u)$, $N_n(u)$ and $N_p(u)$ are the numbers of nucleons, neutrons and protons at parameter u which denotes the rapidity y or transverse momentum p_t , and w_i is 1 for neutrons and -1 for protons, respectively. Shown in Fig. 6 is the rapidity dependence of neutron-proton differential elliptic flow in semicentral and peripheral $^{208}\text{Pb}+^{208}\text{Pb}$ collisions with impact parameters of 5 and 9 fm and at beam energies from 50 to 1000 MeV/nucleon, respectively. It is expected that the neutron-proton differential elliptic flow shows obvious sensitivity to the symmetry energy. This can be understandable since the combined elliptic flow constructively maximizes the effects of the symmetry potential but minimizes the effects of the isoscalar potential similar to that of neutron-proton differential transverse flow proposed by Li [61]. On the other hand, noticing that the neutron-proton differential elliptic flow in midrapidity ($|y/y_{beam}| \leq 0.5$) is hardly affected by the neutron-skin size difference but sensitive to symmetry energy, the transverse momentum dependence of neutron-proton differential elliptic flow of the midrapidity ($|y/y_{beam}| \leq 0.5$) is shown in Fig. 7. It can be found that the transverse momentum dependence

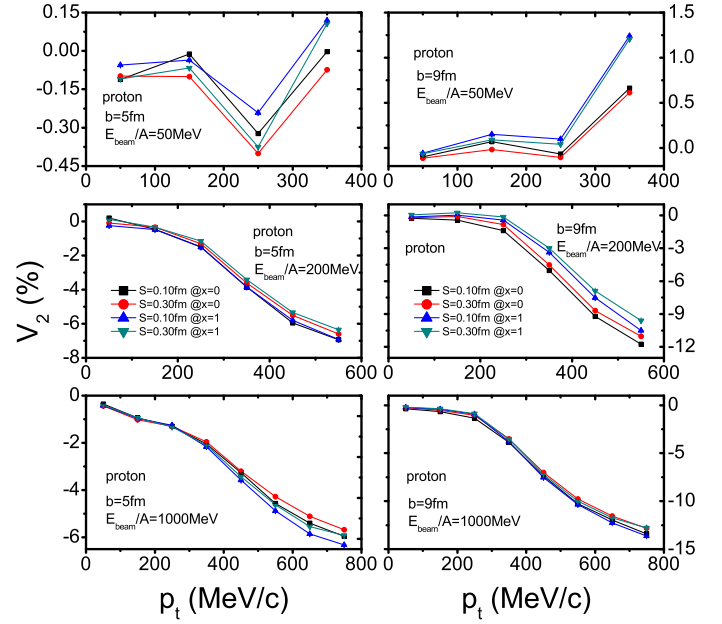


FIG. 5: (Color online) Same as Fig. 4 but for protons.

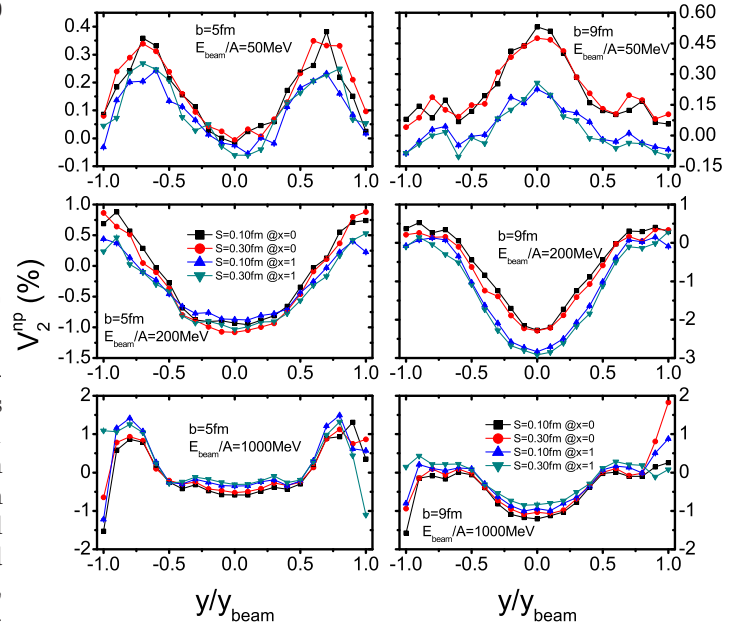


FIG. 6: (Color online) The rapidity dependence of neutron-proton differential elliptic flow in $^{208}\text{Pb}+^{208}\text{Pb}$ collisions with impact parameters of 5 and 9 fm and at beam energies from 50 to 1000 MeV/nucleon, respectively.

of neutron-proton differential elliptic flow is indeed more sensitive to symmetry energy but hardly sensitive to the neutron-skin size difference especially at the lower beam energy.

Another combination of the neutron and proton elliptic flows is the direct difference of them proposed in Ref.

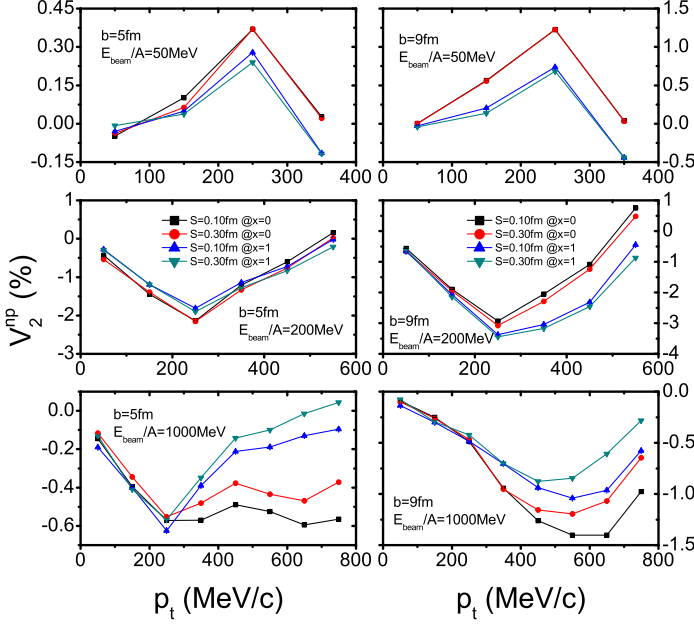


FIG. 7: (Color online) The transverse momentum dependence of neutron-proton differential elliptic flow of the midrapidity ($|y/y_{beam}| \leq 0.5$) in $^{208}\text{Pb}+^{208}\text{Pb}$ collisions with impact parameters of 5 and 9fm and beam energies from 50 to 1000 MeV/nucleon, respectively.

[20, 60] defined as

$$v_2^{n-p}(p_t) = \langle v_2^n(p_t) \rangle - \langle v_2^p(p_t) \rangle, \quad (3)$$

which should also be sensitive to symmetry energy since it is the special case of the neutron-proton differential elliptic flow, i.e., when the neutron and proton have the same multiplicities but different average elliptic flow. Shown in Fig. 8 is the transverse momentum dependence of neutron-proton elliptic flow difference of the midrapidity ($|y/y_{beam}| \leq 0.5$) in semicentral and peripheral $^{208}\text{Pb}+^{208}\text{Pb}$ collisions with impact parameters of 5 and 9fm and at beam energies from 50 to 1000 MeV/nucleon, respectively. It is seen that the transverse momentum dependence of neutron-proton elliptic flow difference is indeed sensitive to symmetry energy but hardly sensitive to the neutron-skin size difference especially at the lower beam energy. These indicate that combination of neutron and proton elliptic flows, i.e., neutron-proton differential elliptic flow and neutron-proton elliptic flow difference, can effectively eliminate the effects of neutron-skin size difference especially at the lower beam energy and thus can be as useful sensitive observables in probing nuclear matter symmetry energy in heavy-ion collisions.

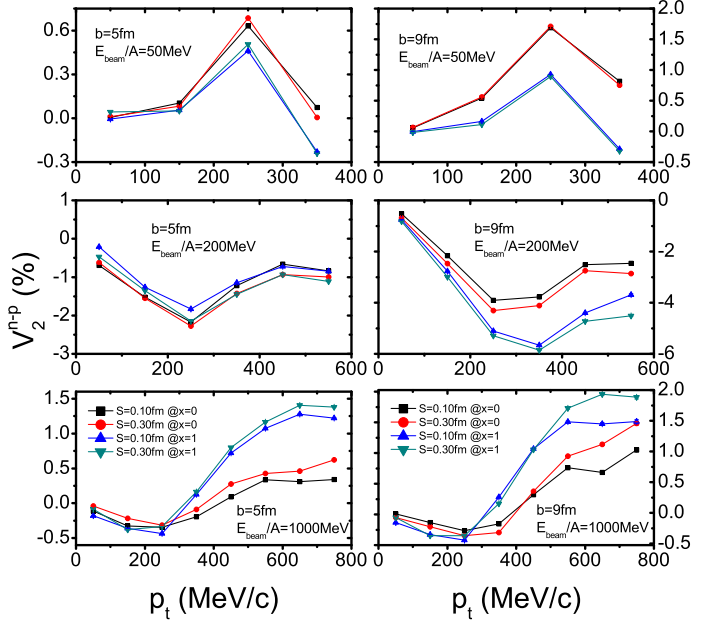


FIG. 8: (Color online) The transverse momentum dependence of neutron-proton elliptic flow difference of the midrapidity ($|y/y_{beam}| \leq 0.5$) in $^{208}\text{Pb}+^{208}\text{Pb}$ collisions with impact parameter of 5 and 9fm and beam energies from 50 to 1000 MeV/nucleon, respectively.

B. The transverse flow

The neutron-proton differential transverse flow as a good tracer of the symmetry potential defined as

$$\begin{aligned} p_x^{n-p}(y) &= \frac{1}{N(y)} \sum_{i=1}^{N(y)} p_x^i(y) w_i \\ &= \frac{N_n(y)}{N(y)} \langle p_x^n(y) \rangle - \frac{N_p(y)}{N(y)} \langle p_x^p(y) \rangle, \end{aligned} \quad (4)$$

was proposed to measure symmetry energy in heavy-ion collisions due to its advantages of combining constructively effects of the symmetry potential on the isospin fractionation and the collective flow [61]. When the neutron and proton have the same multiplicities but different average transverse flow, the neutron-proton differential transverse flow naturally becomes the direct difference of the neutron and proton transverse flows, i.e., the neutron-proton transverse flow difference,

$$p_x^{n-p}(y) = \langle p_x^n(y) \rangle - \langle p_x^p(y) \rangle. \quad (5)$$

Similar to the neutron-proton differential elliptic flow and neutron-proton elliptic flow difference, combination of the neutron and proton transverse flows, i.e., neutron-proton differential transverse flow and neutron-proton transverse flow difference, can effectively eliminate the effects of neutron-skin size difference but keep the effects of symmetry energy especially at the lower beam energy

as shown in Fig. 9. At the beam energies of 200 and 1000MeV/nucleon, the neutron-proton differential transverse flow and/or neutron-proton transverse flow difference are less sensitive to nuclear symmetry energy compared to those at 50MeV/nucleon.

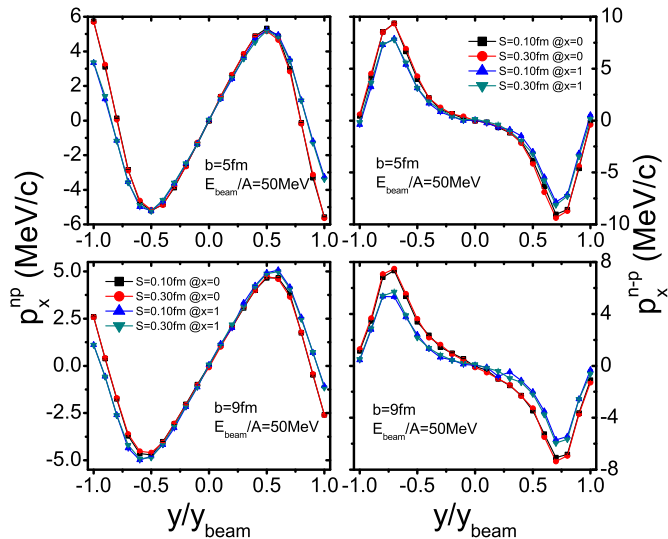


FIG. 9: (Color online) The neutron-proton differential transverse flow (left panel) and neutron-proton transverse flow difference (right panel) in $^{208}\text{Pb}+^{208}\text{Pb}$ collisions with impact parameter of 5 and 9fm and beam energy of 50MeV/nucleon, respectively.

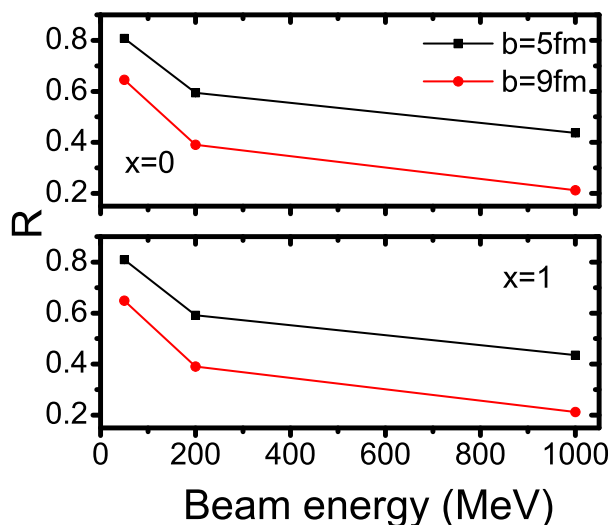


FIG. 10: (Color online) The beam energy and impact parameter dependence of stopping power of all nucleons in $^{208}\text{Pb}+^{208}\text{Pb}$ collisions with the stiff (upper panel) and soft (lower panel) symmetry energy, respectively.

C. The stopping power

Collective flow, generated by pressure gradient of dense nuclear matter formed in heavy ion collision, is closely related to nuclear stopping power. Large stopping power can lead to a remarkable pressure gradient in the compressed nuclear matter. It is also believed that the stopping power governs most of the dissipated energy, the amplitude of large collective motion, the maximum attainable baryon and energy densities, as well as the thermalization of the collision system [62–64]. Two kinds of ratio of transverse to longitudinal quantities are commonly used to measure the degree of stopping; one is the energy-based isotropy ratio, another is the momentum-based isotropy ratio. They are actually the different forms of physics realization of the classical Maxwell distribution assumption [65]. Here, the momentum-based isotropy ratio is employed to measure the degree of stopping, its definition is

$$R = \frac{2}{\pi} \frac{\sum |p_{ti}|}{\sum |p_{zi}|}, \quad (6)$$

where $p_{ti}(p_{zi})$ is the transverse (longitudinal) momentum of nucleon in center of mass system, and the sum runs over all products event by event. It is believed that full stopping is reached when the ratio R reaches the value of 1 [66]; and the superstopping of the ratio $R > 1$ is explained by the preponderance of momentum flow perpendicular to the beam direction [67].

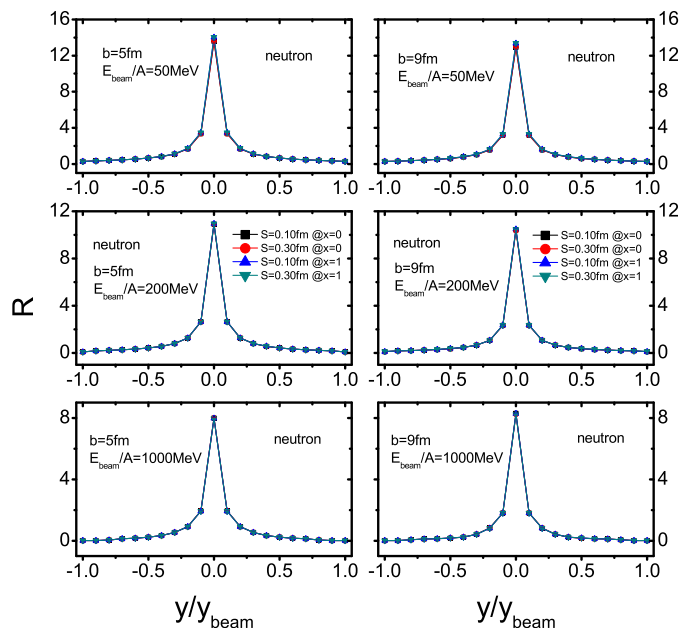


FIG. 11: (Color online) The rapidity dependence of stopping power of neutrons in $^{208}\text{Pb}+^{208}\text{Pb}$ collisions with impact parameter of 5 and 9fm and beam energies from 50 to 1000 MeV/nucleon, respectively.

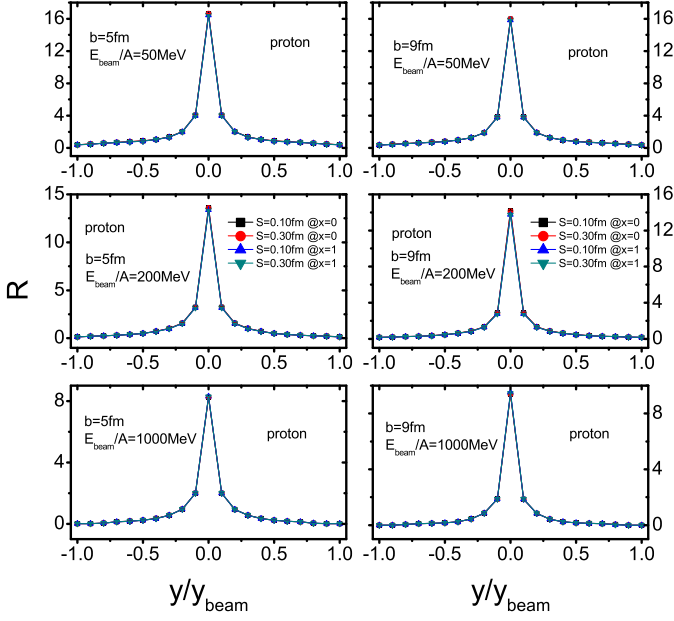


FIG. 12: (Color online) Same as Fig. 11 but for protons.

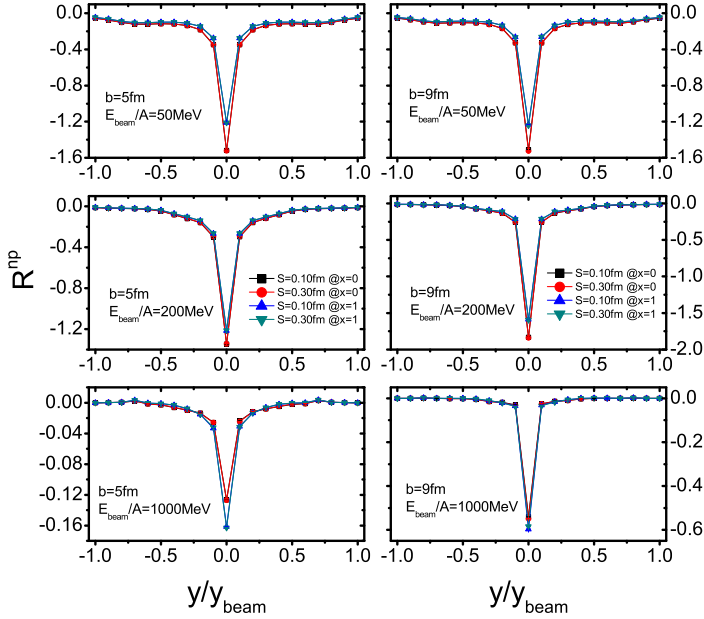


FIG. 13: (Color online) The rapidity dependence of neutron-proton differential stopping power in $^{208}\text{Pb}+^{208}\text{Pb}$ collisions with impact parameter of 5 and 9 fm and beam energies from 50 to 1000 MeV/nucleon, respectively.

Let's first look at the global dependence of the stopping power on beam energy, impact parameter and symmetry energy for a given neutron-skin thickness of 0.1 fm. Shown in Fig. 10 is the beam energy and impact parameter dependence of stopping power of all nucleons in $^{208}\text{Pb}+^{208}\text{Pb}$ collisions with the stiff and soft symmetry

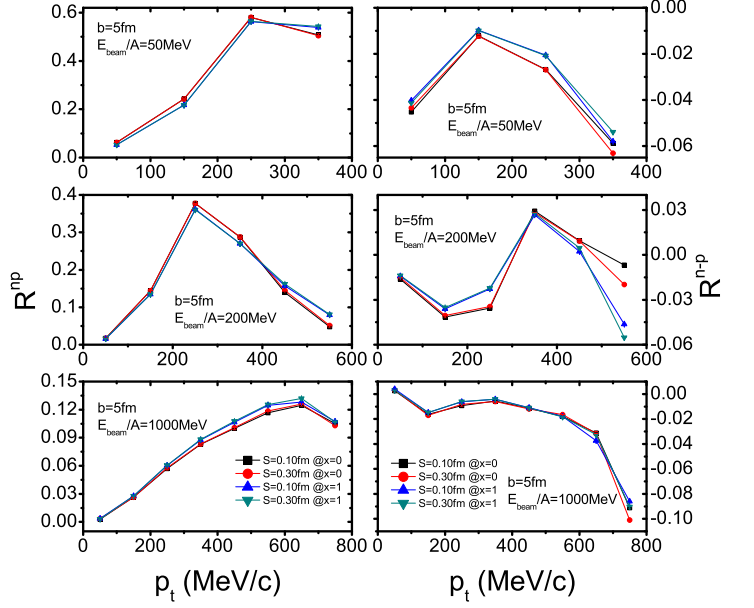


FIG. 14: (Color online) The transverse momentum dependence of neutron-proton differential stopping power (left panel) and neutron-proton stopping power difference (right panel) of the midrapidity ($|y/y_{\text{beam}}| \leq 0.5$) in $^{208}\text{Pb}+^{208}\text{Pb}$ collisions with impact parameter of 5 fm and beam energies from 50 to 1000 MeV/nucleon, respectively.

energy, respectively. It is seen the stopping power of all nucleons is decreasing with the beam energy and impact parameter increasing regardless of the stiff or soft symmetry energy. These are consistent with previous results in Ref. [63, 64]. However, the stopping power of all nucleons is not sensitive to symmetry energy at all. Is the stopping power of neutrons or protons sensitive to symmetry energy? Can the combined stopping power eliminate the influence of neutron-skin size difference of initial colliding nuclei but keep the effect of symmetry energy? To answer these questions, let's first define the neutron-proton differential stopping power R^{np} and neutron-proton stopping power difference R^{n-p} similar to those of combined collective flow as follows,

$$R^{np}(u) = \frac{N_n(u)}{N(u)} \langle R_n(u) \rangle - \frac{N_p(u)}{N(u)} \langle R_p(u) \rangle, \quad (7)$$

$$R^{n-p}(u) = \langle R_n(u) \rangle - \langle R_p(u) \rangle, \quad (8)$$

where $N(u)$, $N_n(u)$ and $N_p(u)$ are the numbers of nucleons, neutrons and protons at parameter u which denotes the rapidity y or transverse momentum p_t , respectively. Shown in Figs. 11, 12 and 13 are the rapidity dependence of stopping power of neutrons, protons and neutron-proton differential stopping power in $^{208}\text{Pb}+^{208}\text{Pb}$ collisions with impact parameters of 5 and 9 fm and at beam energies from 50 to 1000 MeV/nucleon, respectively. It can be found that although the stopping power of neutrons and/or protons does not show obvious sensitivities

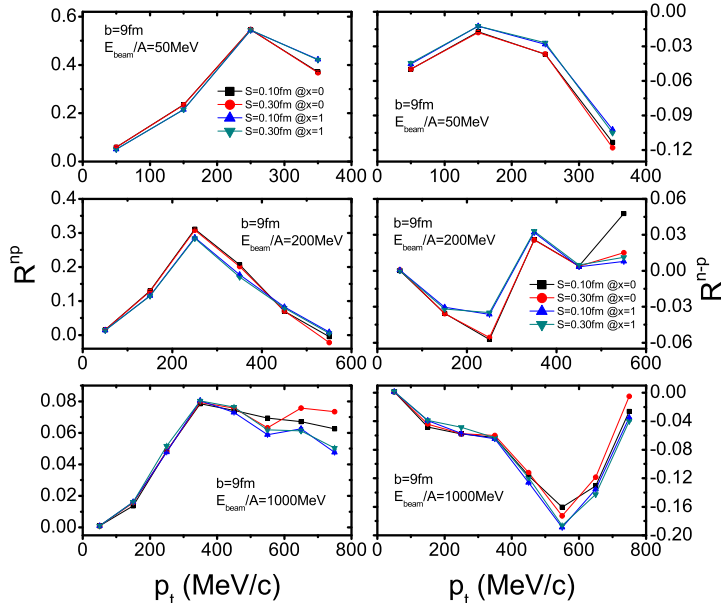


FIG. 15: (Color online) Same as Fig. 14 but with impact parameter of 9fm.

to symmetry energy, the neutron-proton differential stopping power shows obvious sensitivities to symmetry energy especially for midrapidity nucleons and at the lower beam energy. In addition, the neutron-proton stopping power is hardly affected by the neutron-skin size difference of initial colliding nuclei. This is very similar to that of combined transverse and elliptic flows due to their correlation as pointed out in Ref. [62], i.e., flow is generated by pressure gradients established in compressed matter, while the achieved density is connected to the degree of stopping.

Finally, noticing that the midrapidity neutron-proton differential stopping power is obvious sensitive to symmetry energy but hardly affected by the neutron-skin size difference of initial colliding nuclei, the transverse momentum dependence of midrapidity neutron-proton combined stopping power including the neutron-proton differential stopping power and neutron-proton stopping

power difference is shown in Figs. 14 and 15, respectively. It is shown that the transverse momentum dependence of midrapidity neutron-proton combined stopping power shows more obvious sensitivities to symmetry energy but hardly affected by the neutron-skin size difference especially at the lower beam energy.

IV. SUMMARY

In this work by studying the influence of the neutron-skin size of initial colliding nuclei on the collective flow and nuclear stopping power, we have showed how to eliminate the influence of the neutron-skin size difference of initial colliding nuclei in semicentral and peripheral Pb+Pb collisions at beam energies from 50 to 1000 MeV/nucleon, respectively. Noticing that the effects of neutron-skin size on collective flow of neutron and proton are approximately identical except for the additional Coulomb repulsion between protons, it is thus that combination of neutron and proton collective flows, i.e., neutron-proton differential transverse and elliptic flows and neutron-proton transverse and elliptic flow differences, can effectively eliminate the effects of neutron-skin size difference especially at the lower beam energy and thus can be as useful sensitive observables of nuclear matter symmetry energy in heavy-ion collisions. In addition, the combined stopping power including neutron-proton differential stopping power and neutron-proton stopping power difference also shows some sensitivities to symmetry energy but hardly affected by neutron-skin size difference of initial colliding nuclei especially at the lower beam energy.

Acknowledgements

The author is grateful to Profs. B.A. Li, J.Xu and L.W. Chen for their helpful discussions. The author also thanks the help provided by the supporting staff of the High-Performance Computational Science Research Cluster at Texas A&M University-Commerce where partial calculations were done. This work was supported by the National Natural Science Foundation of China under grant No.11405128.

[1] K. Oyamatsu, I. Tanihata, Y. Sugahara, K. Sumiyoshi, and H. Toki, Nucl. Phys. A **634**, 3 (1998).
 [2] B. A. Brown, Phys. Rev. Lett. **85**, 5296 (2000).
 [3] C. J. Horowitz and J. Piekarewicz, Phys. Rev. Lett. **86**, 5647 (2001); Phys. Rev. C **66**, 055803 (2002).
 [4] R. J. Furnstahl, Nucl. Phys. A **706**, 85 (2002).
 [5] H. A. Bethe, Rev. Mod. Phys. **62**, 801 (1990).
 [6] J. M. Lattimer and M. Prakash, Astrophys. J. **550**, 426 (2001).
 [7] L. Engvik, M. Hjorth-Jensen, E. Osnes, G. Bao, and E. Østgaard, Phys. Rev. Lett. **73**, 2650 (1994).
 [8] M. Prakash, T. L. Ainsworth, and J. M. Lattimer, Phys.

Rev. Lett. **61**, 2518 (1988).
 [9] L. W. Chen, V. Greco, C. M. Ko, and B. A. Li, Phys. Rev. Lett. **90**, 162701 (2003).
 [10] B. A. Li, Phys. Rev. C **69**, 034614 (2004).
 [11] H. Muller and B. D. Serot, Phys. Rev. C **52**, 2072 (1995).
 [12] V. Baran, M. Colonna, M. Di Toro, V. Greco, M. Zielinska-Pfabé, and H.H. Wolter, Nucl. Phys. A **703**, 603 (2002).
 [13] L. W. Chen, C. M. Ko, and B. A. Li, Phys. Rev. C **68**, 017601 (2003).
 [14] L. Shi and P. Danielewicz, Phys. Rev. C **68**, 064604 (2003).

- [15] L. Scalone, M. Colonna, and M. Di Toro, Phys. Lett. B **461**, 9 (1999).
- [16] B. A. Li, A. T. Sustich, and B. Zhang, Phys. Rev. C **64**, 054604 (2001).
- [17] B. A. Li, Phys. Rev. Lett. **88**, 192701 (2002).
- [18] T. Gaitanos, M. Di Toro, S. Typel, V. Baran, C. Fuchs, V. Greco, and H. H. Wolter, Nucl. Phys. A **732**, 24 (2004).
- [19] P. Danielewicz, R. A. Lacey, P. B. Gossiaux, C. Pinkenburg, P. Chung, J. M. Alexander, and R. L. McGrath, Phys. Rev. Lett. **81**, 2438 (1998).
- [20] V. Baran, M. Colonna, V. Greco, and M. Di toro, Phys. Rep. **410**, 335 (2005).
- [21] B. A. Li, L. W. Chen, and C. M. Ko, Phys. Rep. **464**, 113 (2008).
- [22] H. Stöcker and W. Greiner, Phys. Rep. **137**, 277 (1986).
- [23] W. Cassing, V. Metag, U. Mosel, and K. Niita, Phys. Rep. **188**, 363 (1990).
- [24] J. Harris and B. Müller, Annu. Rev. Nucl. Part. Sci. **46**, 71 (1996).
- [25] C. M. Ko and G. Q. Li, J. Phys. G **22**, 1673 (1996).
- [26] B. A. Li, C. M. Ko, and W. Bauer, Int. J. Mod. Phys. E **7**, 147 (1998).
- [27] M. Di Toro, V. Baran, M. Colonna, G. Fabbri, A. B. Larionov, S. Maccarone, and S. Scalone, Prog. Part. Nucl. Phys. **42**, 125 (1999).
- [28] X. Y. Sun, D. Q. Fang, Y. G. Ma, X. Z. Cai, J. G. Chen, W. Guo, W. D. Tian, H. W. Wang, Phys. Lett. B **682**, 396 (2010).
- [29] Z. T. Dai, D. Q. Fang, Y. G. Ma, X. G. Cao, G. Q. Zhang, Phys. Rev. C **89**, 014613 (2014).
- [30] B. A. Li, C. B. Das, S. Das Gupta, and C. Gale, Phys. Rev. C **69** (2004) 011603(R); Nucl. Phys. A **735** (2004) 563.
- [31] P. Danielewicz, Ann. Phys. **152**, 239 (1984).
- [32] W. Botermans, R. Malfliet, Phys. Rep. **198** 115 (1990).
- [33] G. F. Wei, B. A. Li, J. Xu, and L. W. Chen, Phys. Rev. C **90**, 014610 (2014).
- [34] L. Ou and B. A. Li, Phys. Rev. C **84**, 064605 (2011).
- [35] C. Gale, G. Bertsch, and S. Das Gupta, Phys. Rev. C **35**, 1666 (1987).
- [36] G. M. Welke, M. Prakash, T. T. S. Kuo, S. Das Gupta, and C. Gale, Phys. Rev. C **38**, 2101 (1988).
- [37] C. Gale, G. M. Welke, M. Prakash, S. J. Lee, and S. Das Gupta, Phys. Rev. C **41**, 1545 (1990).
- [38] P. Danielewicz, Nucl. Phys. A **673**, 375 (2000).
- [39] V. Greco, A. Guarnera, M. Colonna, and M. Di Toro, Phys. Rev. C **59**, 810 (1999).
- [40] C. B. Das, S. Das Gupta, C. Gale, and B. A. Li, Phys. Rev. C **67**, 034611 (2003).
- [41] L. W. Chen, C. M. Ko, and B. A. Li, Phys. Rev. C **69**, 054606 (2004).
- [42] J. Rizzo, M. Colonna, M. Di Toro, and V. Greco, Nucl. Phys. A **732**, 202 (2004).
- [43] J. Xu, L. W. Chen, B. A. Li, and H. R. Ma, Phys. Rev. C **75**, 014607 (2007).
- [44] J. Xu, L. W. Chen, B. A. Li, and H. R. Ma, Phys. Lett. B **650**, 348 (2007).
- [45] J. Xu, L. W. Chen, B. A. Li, and H. R. Ma, Phys. Rev. C **77**, 014302 (2008).
- [46] L. W. Chen, C. M. Ko, and B. A. Li, Phys. Rev. Lett. **94**, 032701 (2005).
- [47] Z. G. Xiao, B. A. Li, L. W. Chen, G. C. Yong, and M. Zhang, Phys. Rev. Lett. **102**, 062502 (2009).
- [48] Z. Q. Feng, G. M. Jin, Phys. Lett. B **683**, 140 (2010).
- [49] J. Xu, Z. Martinot, and B. A. Li, Phys. Rev. C **86**, 044623 (2012).
- [50] L. W. Chen, B. J. Cai, C. M. Ko, B. A. Li, C. Shen, and J. Xu, Phys. Rev. C **80**, 014322 (2009).
- [51] L. W. Chen, C. M. Ko, B. A. Li, and J. Xu, Phys. Rev. C **82**, 024321 (2010).
- [52] E. Friedman, Nucl. Phys. A **896**, 46 (2012).
- [53] S. Abrahamyan *et al.*, Phys. Rev. Lett. **108**, 112502 (2012).
- [54] F. J. Fattoyev and J. Piekarewicz, Phys. Rev. Lett. **111**, 162501 (2013).
- [55] H. C. Song, S. A. Bass, U. Heinz, T. Hirano, and C. Shen, Phys. Rev. Lett. **106**, 192301 (2011).
- [56] P. Danielewicz, R. Lacey, W.G. Lynch, Science **298**, 1592 (2002).
- [57] Y. M. Zheng, C. M. Ko, B. A. Li, and B. Zhang, Phys. Rev. Lett. **83**, 2534 (1999).
- [58] K. S. Vinayak, and S. Kumar, Eur. Phys. J. A **47**, 144 (2011).
- [59] W. Trautmann and H. H. Wolter, Int. J. Mod. Phys. E **21**, 1230003 (2012).
- [60] V. Giordano, M. Colonna, M. Di Toro, V. Greco, and J. Rizzo, Phys. Rev. C **81**, 044611 (2010).
- [61] B. A. Li, Phys. Rev. Lett. **85**, 4221 (2000).
- [62] A. Andronic, J. Lukasik, W. Reisdorf, and W. Trautmann, Eur. Phys. J. A **30**, 31 (2006).
- [63] X. F. Luo, X. Dong, M. Shao, K. J. Wu, C. Li, H. F. Chen, and H. S. Xu, Phys. Rev. C **76**, 044902 (2007).
- [64] G. Lehaut *et al.*, Phys. Rev. Lett. **104**, 232701 (2010).
- [65] G. Q. Zhang, Y. G. Ma, X. G. Cao, C. L. Zhou, X. Z. Cai, D. Q. Fang, W. D. Tian, and H. W. Wang, Phys. Rev. C **84**, 034612 (2011).
- [66] H. Ströbele *et al.*, Phys. Rev. C **27**, 1349 (1983).
- [67] R. E. Renfordt *et al.*, Phys. Rev. Lett. **53**, 763 (1984).